# Nonlinearities in Balanced Armature Transducers[1]

Wolfgang Klippel
KLIPPEL GmbH, Dresden, 01309, Germany

Electromagnetic transducers using a balanced armature play an important role in hearing aids and in-ear headphones because they generate required sound output at high efficiency. This paper investigates the transfer behavior at high amplitudes and develops a lumped parameter model of this transducer that considers the nonlinearities caused by the geometry and material properties. This model is a basis for optimal transducer design, adjusting the armature in production and actively cancelling the nonlinear distortion through nonlinear, adaptive control.

## I. INTRODUCTION

Most loudspeakers, headphones and other electro-acoustical devices use an electro-dynamical transducer with a moving voice coil in a static magnetic field. Models have been developed for this kind of transducer which provide sufficient accuracy for measurement and control application [1].

Electro-magnetic transducers use a coil at a fixed position and a moving armature connected via a driving pin to a diaphragm [2]. This kind of transducer has some desired properties (e.g. high efficiency) that are not found in electro-dynamical transducers [3]. The nonlinearities inherent in the electro-magnetic principle are a source of signal distortion [4]. This disadvantage can be partly reduced by using an armature balanced in a magnetic field generated by additional magnets as shown in Figure 1.

An accurate model of the balanced armature transducer is required to get a deeper insight into the physical causes and to predict the large signal performance for any input signal. Hunt [2] developed a nonlinear model that describes the electro-magnetic transducer by an electrical equivalent circuit comprising lumped elements. The inherent nonlinearities are represented by inductance $L(\xi)$, transduction factor $T(\xi)$ and magnetic stiffness $K_{mag}(\xi)$ depending on the displacement $\xi$ of the armature. All parameters are derived from the geometry of an ideal transducer having a magnetic material without saturation and hysteresis. This paper investigates the validity of those assumptions and presents an extended model that considers the dominant nonlinearities found in real BA-transducers.

[1] This paper is an amended version of reference [10] with small changes in equations (5) and (24).

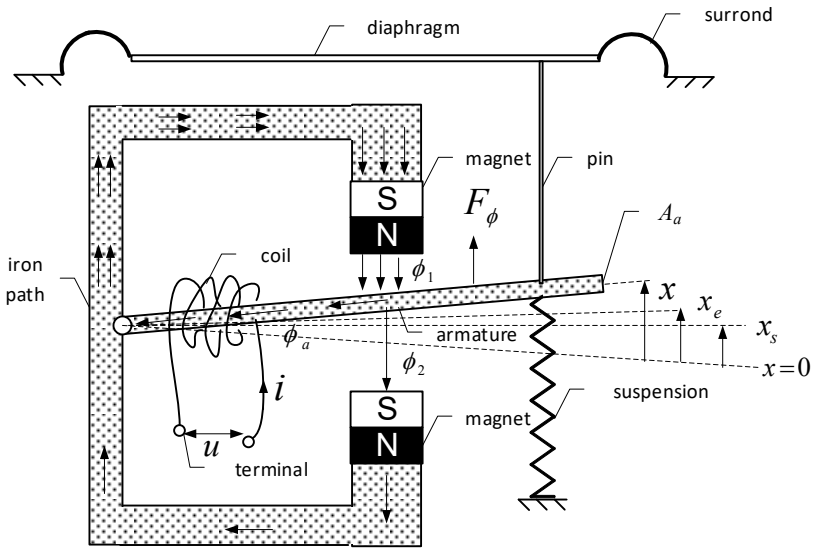


*Figure 1. Sectional view of a balanced-armature transducer*

## II. GEOMETRICAL NONLINEARITY

The derivation of the theory is illustrated on the balanced-armature device shown in Figure 1. An armature with a cross sectional area $A_a$ is placed between two magnets, generating an upper and lower gap which are closed by a rear air on path. A coil placed at a fixed position generates a magneto-motive force $Ni$ in the armature depending on the number $N$ of wire turns and input current $i$ at the terminals. The armature is connected via a driving rod to a diaphragm. The diaphragm and an optional mechanical suspension determine the initial rest position of the armature $x$=0.

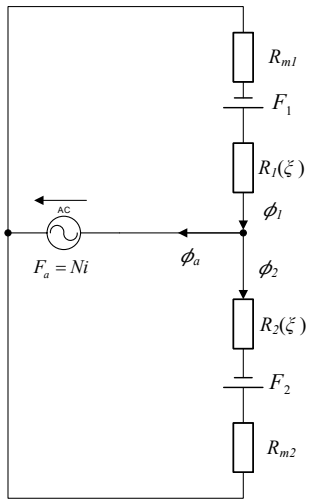


*Figure 2. Simplified magnetic circuit of the balanced-armature transducer considering geometrical nonlinearity only*

The conventional model, as described by F.V. Hunt [2] and J. Jensen [6], is based on the simplified magnetic circuit shown in
Figure *2*.tif. It is assumed that the two magnets have the same magneto-motive force

$$F_m = F_1 = F_2 \qquad (1)$$

and the internal reluctance of the magnet is represented by the same value in the upper and lower path

$$R_m = R_{m1} = R_{m2} = \frac{l_M}{\mu_0 \mu_r A_M} = \frac{D_M}{\mu_0 A_a} \tag{2}$$

using the permeability $\mu_0$ of air, equivalent air gap length $D_M$ representing the permanent magnet with cross sectional area $A_M$, geometrical length $l_M$ and relative permeability $\mu_r$. It is assumed that the area of the magnet equals the area of the air gap:

$$A_m = A_g = A \tag{3}$$

The point $x$=0 is defined as initial armature rest position without applying a magneto-motive force ($F_m$=0) or an input current ($i$=0). It is also assumed that this point $x$=0 is equal to the symmetry point $x_s$=0, which generates the same length $D$ of the upper and lower air gap. After magnetizing the two magnets ($F_m$>0), the armature is moved to the equilibrium position $x_e$. The conventional modeling [2] assumes that the equilibrium position also equals the initial rest position $x_e$=$x_s$=0. An input current $i$≠0 causes an additional displacement $\xi$=$x$-$x_e$ of the armature which generates the desired acoustical output.

Under those assumptions, the magnet fluxes $\phi_1$ and $\phi_2$ in the upper and lower path, respectively, can be described by

$$\phi_1 = \frac{F_m + Ni}{R_1(\xi) + R_m} \tag{4}$$

$$\phi_2 = \frac{F_m - Ni}{R_2(\xi) + R_m} \tag{5}$$

using the nonlinear reluctances $R_1(\xi)$ and $R_2(\xi)$ representing the upper and lower air gap, respectively, which can be calculated as

$$R_1(\xi) + R_m = \frac{D + D_m - \xi}{\mu_0 A} = \frac{D_{eff} - \xi}{\mu_0 A} \tag{6}$$

$$R_2(\xi) + R_m = \frac{D + D_m + \xi}{\mu_0 A} = \frac{D_{eff} + \xi}{\mu_0 A} \tag{7}$$

with the effective air gap length $D_{eff}$ considering the magnet length $D_m$.

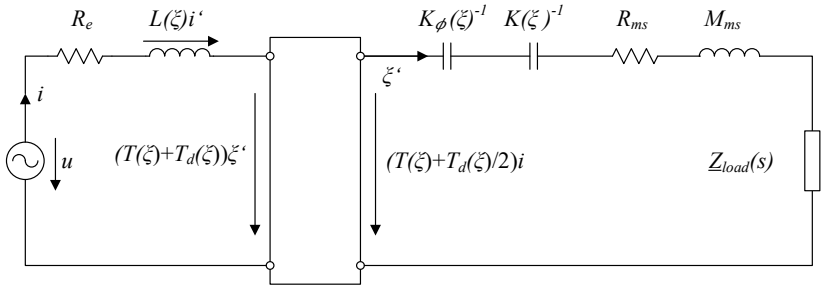


*Figure 3. Equivalent circuit of the conventional modeling considering the geometrical nonlinearity at the equilibrium point xe*

Following the derivation described in greater detail by Jensen [6] leads to the equivalent circuit in Figure 3. corresponding to a voltage equation

$$u = R_e i + L(\xi)\frac{di}{dt} + \left(T(\xi) + T_d(\xi, i)\right)\frac{d\xi}{dt} \tag{8}$$

and a force equation

$$\left(T(\xi,i)+T_d(\xi,i)/2\right)i=\left(K(\xi)-K(0)\right)\xi-K_\phi(\xi)\xi + \mathrm{L}^{-1}\left\{\underline{Z}_m(\xi,s)s\right\}*\xi \tag{9}$$

using the inverse Laplace transformation $\mathrm{L}^{-1}\{\}$ and the convolution operator * to consider the mechanical impedance:

$$\underline{Z}_m(s)=\frac{K(0)}{s}+R_{ms}+M_{ms}s+\underline{Z}_{load}(s) \tag{10}$$

The linear lumped parameters of the transducer are an electrical DC coil resistance $R_e$, a moving mass $M_{ms}$, a mechanical resistance $R_{ms}$ representing the losses in the mechanical system and the impedance $Z_{load}(s)$ of the mechanic and acoustic load.

The nonlinear parameters comprise an inductance depending on displacement

$$L(\xi)=\frac{2\mu_0 AN^2}{D_{eff}}\frac{D_{eff}^2}{D_{eff}^2-\xi^2} \tag{11}$$

a transduction factor coupling the electrical with mechanical side expressed as

$$T(\xi)=2\mu_0 ANF_m\frac{{D_{eff}}^2+\xi^2}{\left({D_{eff}}^2-\xi^2\right)^2} \tag{12}$$

a second transduction factor depending on displacement and current

$$T_d(\xi,i)=\frac{4\mu_0 AD_{eff}N^2\xi i}{\left({D_{eff}}^2-\xi^2\right)^2} \tag{13}$$

a magnetic stiffness expressed

$$K_\phi(\xi)=\frac{2\mu_0 AD_{eff}F_m^2}{\left({D_{eff}}^2-\xi^2\right)^2} \tag{14}$$

and the stiffness $K(\xi)$ of the mechanical suspension, which is also found in moving coil transducers.

The displacement varying reluctances $R_1(\xi)$ and $R_2(\xi)$ generate a characteristic term $D_{eff}^2 - \xi^2$ in the denominator of Eqs. (11) - (14) that generates a symmetrical increase of the nonlinear parameters for positive and negative displacement.

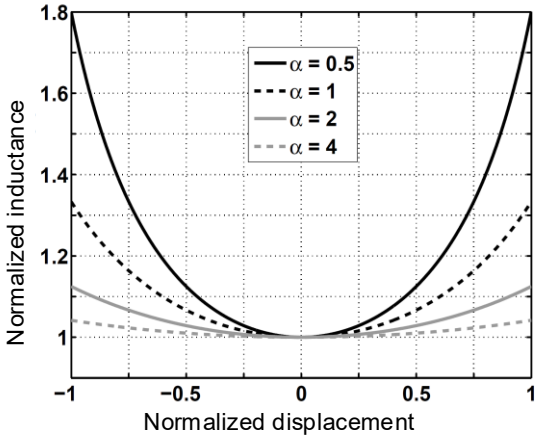


*Figure 4. Normalized coil inductance L(ξ)/L(ξ=0) versus normalized displacement ξ/D based on the conventional model that only considers the geometrical nonlinearity for different ratios α= Dm/D between air gap length D and equivalent air gap length of the magnet Dm (Jensen 6 ).*

## A. Insufficiencies of the Geometrical Model

Klippel [5] and Jensen [6] found a significant discrepancy between the predicted behavior based on the conventional model and the behavior of real BA-transducers. For example, Figure 4. shows an increase of the normalized inductance $L(\xi)/L(\xi=0)$ for any displacement $\xi$ as calculated by Jensen [6]. The geometrical nonlinearity becomes stronger for a smaller ratio α corresponding to a smaller reluctance $R_m$ in the magnets.

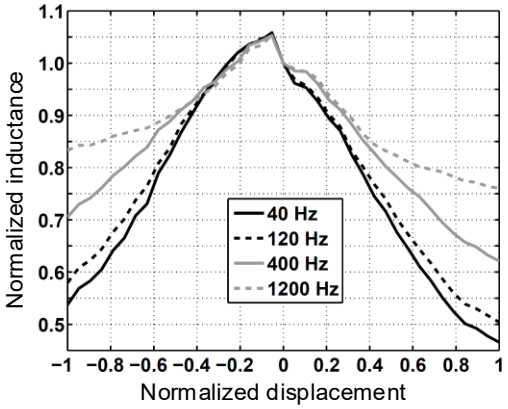


*Figure 5. Normalized coil inductance L(ξ)/L(ξ=0) versus normalized DC displacement ξ/D of the clamped armature derived from electrical input impedance measured at selected frequencies (Jensen 6).*

However, in practical measurements of typical BA-transducers, Jensen [6] found a significant decrease of the inductance as shown in Figure 5.tif, which is the exact opposite of the predicted behavior in Figure 4.tif. Klippel [5] performed similar experiments on BA-transducers in which the armature was clamped at a fixed displacement $\xi$ and excited with a broadband stimulus containing a variable DC component and found that the inductance $L(\xi,i)$ decreases not only with displacement but also with current $i$. Those observations are indications of the saturation of the armature and other soft iron material in the magnetic path. Although those facts have not been incorporated in the conventional modeling, it is known in the industry and already used in practical design. Thompsen [7] disclosed small modifications on the armature to use the nonlinear saturation for compensating the geometrical nonlinearity and reducing the distortion in the acoustical output signal.

There are further shortcomings of the conventional model: The assumption $x_e=x_s=0$ generates a symmetrical curve shape in the inductance $L(\xi)$, as shown in Figure 4., that can only explain the generation of 3rd-order and other odd-order harmonic or intermodulation distortion [4]. Real transducers generate 2nd-order distortion that is related to asymmetries in the nonlinear curve shape, which is also clearly visible in the example shown in Figure 5.tif. Considering an asymmetrical curve shape of the nonlinear motor and suspension parameters shown in Figure 3. requires a reliable theory for predicting the equilibrium point $x_e$, which can be different from the initial rest position $x=0$ of the suspension without magnets and the symmetry point $x_s$. In other words, a model is required that describes the absolute position $x$ of the armature.

Another objective is to increase the model power, achieving greater accuracy while keeping the model complexity as small as possible. This can be accomplished by useful approximations and detailed discussions of their validity.

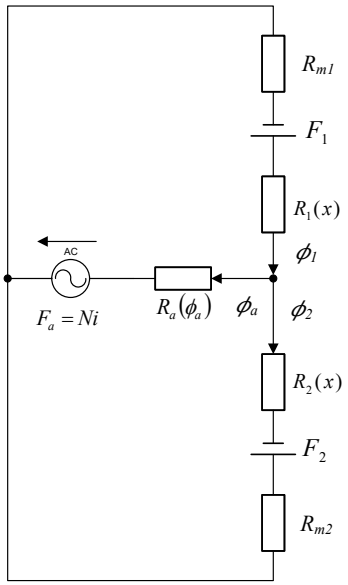


*Figure 6. Magnetic circuit of the balanced-armature transducer using a nonlinear reluctance Ra(ϕa) to consider the saturation of the soft iron armature material.*

## III. MODEL WITH SATURATION

The decrease of the measured inductance $L(\xi)$ with rising displacement $\xi$ can be explained by a nonlinear reluctance $R_a(\phi_a)$ representing the armature in the magnetic circuit as shown in Figure 6. depending on the magnetic flux $\phi_a$ expressed as:

$$\phi_a = \phi_1 - \phi_2 \tag{15}$$

Assuming that the two magnets are generating the same magneto-motive force $F_m$ and have the same internal magnetic reluctance $R_m$ as introduced in section II, the fluxes $\phi_1$ and $\phi_2$ in the upper and lower air gap, respectively, can be expressed as follows:

$$\phi_1 = \frac{F_m + Ni}{R_1(x) + R_m} - \frac{R_a(\phi_a)}{R_1(x) + R_m}\phi_a \tag{16}$$

$$\phi_2 = \frac{F_m - Ni}{R_2(x) + R_m} + \frac{R_a(\phi_a)}{R_1(x) + R_m}\phi_a \tag{17}$$

The reluctances in the denominator of Eqs. (16) and (17) can be modeled as

$$R_1(x) + R_m = \frac{D - (x - x_s) + l_m / \mu_r}{\mu_0 A} = \frac{D_{eff} - (x - x_s)}{\mu_0 A} \tag{18}$$

$$R_2(x) + R_m = \frac{D + (x - x_s) + l_m / \mu_r}{\mu_0 A} = \frac{D_{eff} + (x - x_s)}{\mu_0 A} \tag{19}$$

with the initial rest position $x$=0 and the symmetry point $x_s$ defined as the position where $R_1(x)$=$R_2(x)$ for $i$=0.

According to Eq. (15) the flux in the armature can be calculated as

$$\begin{aligned}\phi_a &= \phi_1 - \phi_2 \\ &= \frac{F_m + Ni}{R_1(x) + R_m} - \frac{F_m - Ni}{R_2(x) + R_m} \\ &\quad - \left( \frac{1}{R_1(x) + R_m} + \frac{1}{R_2(x) + R_m} \right) \phi_a R_a(\phi_a) \\ &= \frac{2\mu_0 A}{D_{eff}{}^2 - (x - x_s)^2} \begin{pmatrix} ND_{eff} i + F_m (x - x_s) \\ -D_{eff} \phi_a R_a(\phi_a) \end{pmatrix} \\ &= f_x(x,i) \frac{2\mu_0 A}{D_{eff}^2} \left( ND_{eff} i + F_m (x - x_s) \right)\end{aligned} \tag{20}$$

with the nonlinear flux function

$$f_x(x,i) = \frac{1}{1 - \left( \frac{x - x_s}{D_{eff}} \right)^2 + \frac{2\mu_0 A}{D_{eff}} R_a(\phi_a(x,i))} \tag{21}$$

depending on the armature position $x$ and the input current $i$.

The flux function $f_x(x,i)$ is always positive and becomes unity for $x=x_s$ and vanishing current $i$. The first nonlinear term in the denominator in Eq. (21) represents the geometrical nonlinearity of the transducer and generates high values of $f_x(x,i)$ when the distance $|x\text{-}x_s|$ approaches $D_{eff}$ and the reluctance $R_a(\phi_a)$ is low. The second nonlinear term in the denominator represents the saturation and becomes dominant in most BA-transducers

$$\frac{2\mu_0 A}{D_{eff}} R_a(\phi_a(x,i)) > \left( \frac{x - x_s}{D_{eff}} \right)^2 \tag{22}$$

and reduces the value of the flux function for rising flux $\phi_a$.

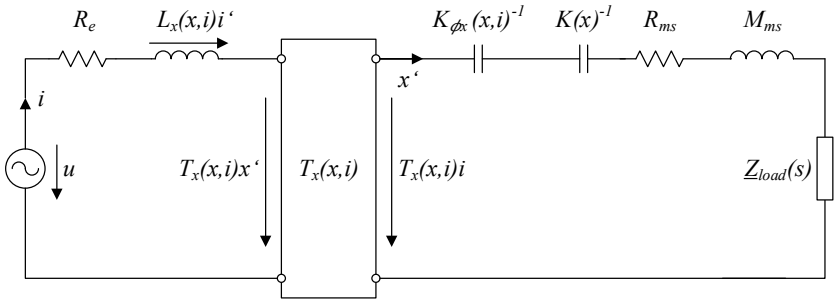


*Figure 7. Advanced lumped parameter model of the BA-transducer considering the geometrical nonlinearity as function of the absolute position x and the saturation of the armature*

## A.Electrical Part

The electrical mesh on the left-hand side of the equivalent circuit in Figure 7. corresponds to

$$\begin{aligned}u &= R_e i + N \frac{d\phi_a}{dt} \\ &= R_e i + N \frac{\partial \phi_a}{\partial i} \frac{di}{dt} + N \frac{\partial \phi_a}{\partial x} \frac{dx}{dt} \\ &= R_e i + L_x(x,i) \frac{di}{dt} + T_x(x,i) \frac{dx}{dt}\end{aligned} \tag{23}$$

comprising nonlinear inductance clamped at position $x$

$$L_x(x,i) = L_s \left[ \begin{array}{l} f_x(x,i) \\ +\left( i + \dfrac{F_m(x-x_s)}{ND_{eff}} \right) \dfrac{\partial f_x(x,i)}{\partial i} \end{array} \right] \approx L_s f_x(x,i) \tag{24}$$

with linear inductance parameter $L_S$ measured with small current $i$ and an armature clamped at the symmetry point $x_s$ expressed as

$$L_s = L_x(x_s, i=0) = \frac{2\mu_0 N^2 A}{D_{eff}} \tag{25}$$

and the electro-magnetic transduction factor

$$T_x(x,i) = \frac{2\mu_0 NAF_m}{D_{eff}^2} \left[ \begin{array}{l} f_x(x,i) \\ +\left( \dfrac{ND_{eff}}{F_m} i + (x-x_s) \right) \dfrac{\partial f_x(x,i)}{\partial x} \end{array} \right] \approx T_x(x_s,0) f_x(x,i) = \lambda L_s f_x(x,i) \tag{26}$$

with a motor characteristic:

$$\lambda = \frac{F_m}{ND_{eff}} \tag{27}$$

The approximations in Eqs. (24) and (26) are useful for modelling BA-transducers with nonlinear saturation because the partial derivative $\partial f_x(x,i)/\partial x$ decreases with rising distance ($x$-$x_s$) and rising current $i$. If the saturation is negligible, the exact solution in Eqs. (24) and (26) corresponds with the derivation presented in section II.

## B. Mechanical Driving Force

The total driving force generated at the armature due to the fluxes $\phi_1$ and $\phi_2$ in the upper and lower air gap can be calculated as:

$$F_\phi = \frac{\phi_1^2 - \phi_2^2}{2\mu_0 A} = \frac{(\phi_1 + \phi_2)\phi_a}{2\mu_0 A} \tag{28}$$

The sum of the fluxes $\phi_1+\phi_2$ in both air gaps can be expressed by the following equation:

$$\begin{aligned} \phi_1 + \phi_2 &= \frac{F_m + Ni}{R_1(x) + R_m} - \frac{F_m - Ni}{R_2(x) + R_m} \\ &\quad + \left( \frac{1}{R_2(x) + R_m} - \frac{1}{R_1(x) + R_m} \right) \phi_a R_a(\phi_a) \\ &= \frac{2\mu_0 A}{D_{eff}^2 - (x-x_s)^2} \left( \begin{array}{l} Ni(x-x_s) \\ +D_{eff} F_m \\ -(x-x_s)\phi_a R_a(\phi_a) \end{array} \right) \end{aligned} \tag{29}$$

Using Eq. (20) to replace the term

$$\phi_a R_a(\phi_a) = \left( 1 - f_x(x,i) \left( 1 - \frac{(x-x_s)^2}{D_{eff}^2} \right) \right) \times \left( Ni + \frac{F_m(x-x_s)}{D_{eff}} \right) \tag{30}$$

in Eq. (29) gives

$$\phi_1+\phi_2=\frac{2\mu_0 A}{D_{eff}}\left[\begin{array}{l}F_m-f_x(x,i)\dfrac{(x-x_s)}{D_{eff}}\\ \times\left(Ni+\dfrac{F_m(x-x_s)}{D_{eff}}\right)\end{array}\right]\approx\frac{2\mu_0 A}{D_{eff}}F_m \tag{31}$$

in which the first term is independent of current and armature position. It is usually dominant in BA-transducers with saturation as discussed already in section A.

Inserting Eqs. (31) and (20) in Eq. (28) gives the total driving force expressed as

$$\begin{aligned}F_\phi &= f_x(x,i)\frac{2\mu_0 A}{D_{eff}^2}\left(ND_{eff}i+F_m(x-x_s)\right)\\ &\times\frac{1}{D_{eff}}\left[\begin{array}{l}F_m-f_x(x,i)\dfrac{(x-x_s)}{D_{eff}}\\ \times\left(Ni+\dfrac{F_m(x-x_s)}{D_{eff}}\right)\end{array}\right]\\ &=-K_{\phi x}(x,i)(x-x_s)+T_{m,F}(x,i)i+T_{m,i}(x,i)i\\ &\approx -K_{\phi x}(x,i)(x-x_s)+T_x(x,i)i\end{aligned} \tag{32}$$

using transduction factor $T_x(x,i)$ introduced in Eq. (26).

The first term in Eq. (32) can be interpreted as a restoring force of a magnetic stiffness which can be approximated as

$$\begin{aligned}K_{\phi x}(x,i)&=\frac{2\mu_0 A}{D_{eff}^3}F_m{}^2 f_x(x,i)\\ &\left(1+f_x(x,i)\frac{(x-x_s)^2}{D_{eff}^2}\right)\\ &\approx-\lambda^2 L_s f_x(x,i)\end{aligned} \tag{33}$$

under the condition that the saturation generates a falling flux function $f_x(x,i)$ for rising distances $|x\text{-}x_s|$. Under the same condition, the transduction coefficient $T_{m,F}$ can be approximated as

$$\begin{aligned}T_{m,F}(x,i)&=\frac{2\mu_0 AF_m N}{D_{eff}^2}f_x(x,i)\\ &\times\left(1+2f_x(x,i)\frac{(x-x_s)^2}{D_{eff}{}^2}\right)\\ &\approx\lambda L_s f_x(x,i)\end{aligned} \tag{34}$$

and the second current dependent transduction coefficient $T_{m,i}$ becomes negligible:

$$T_{m,i}(x,i)=\frac{2\mu_0 AN}{D_{eff}^3}f_x^2(x,i)(x-x_s)i\approx 0 \tag{35}$$

## IV. INTERPRETATION

The extended model represented by an equivalent circuit shown in Figure 7. uses the same elements as in the conventional model in Figure 3. The nonlinear elements inductance $L_x(x,i)$, transduction factor $T_x(x,i)$ and magnetic stiffness $K_{\phi x}(x,i)$ depend via the same flux function $f_x(x,i)$ on the input current $i$ and position $x$. Considering the approximations for the nonlinear parameters, the voltage equation can be expressed as

$$u = R_e i + L_s f_x(x,i)\frac{di}{dt} + \lambda L_s f_x(x,i)\frac{dx}{dt} \tag{36}$$

and force equation becomes:

$$\lambda L_s f_x(x,i) i = \big(K(x) - K(0)\big)x - \lambda^2 L_s f_x(x,i)\big(x - x_s\big) + \mathrm{L}^{-1}\big\{\underline{Z}_m(s)s\big\} * x \tag{37}$$

Thus, the flux function $f_x(x,i)$ and the mechanical stiffness $K(x)$ are the dominant nonlinearities in BA-transducers.

### A. Nonlinear Flux Function

The flux function $f_x(x,i)$ can be approximated by a series expansion

$$f_x(x,i) = \frac{1}{1 - \left(\frac{x - x_s}{D}\right)^2 + \sum_{k=1}^{K} s_k \left| i + s_x \left(\frac{x - x_s}{D}\right)\right|^k} \tag{38}$$

with the coefficients $s_k$ describing the saturation of the magnetic material and the parameter $s_x$ describing the dependency on armature position $x$. The first nonlinear term in the denominator represents the geometrical nonlinearity of the transducer and generates high values of $f_x(x,i)$ when $x$-$x_s$ approaches $\pm D$ and the saturation is negligible ($s_k \approx 0$ for all $k$).

The second nonlinear term in the denominator represents the saturation and becomes dominant in most transducers. If the parameter $s_x$ is high, the saturation in the armature can partly compensate the effect of the geometrical nonlinearity in the first nonlinear term of the denominator.

### B. Symmetry Point

If the magneto-motive forces of the two magnets are identical, as assumed in section III, the symmetry point $x_s$ corresponds to the armature position in which the distance to the upper and lower magnets is equal. At this point the flux function in Eq. (38) becomes the maximum value $f_x(x=x_s, i=0)=1$ and shows a symmetrical decay for positive and negative displacement if the input current is zero. However, the symmetry point $x_s$ in Eq. (38) can also be used for representing other asymmetries in the magnetic circuit such as different size and magnetization of the two magnets.

### C. Equilibrium Rest Position

The armature rest position $x_e$ corresponds to the equilibrium between the mechanical restoring force of the suspension and the electro-magnetic attraction force

$$K(x_e)x_e + K_m(x_e,0)\left(x_e - x_s\right) \overset{!}{=} 0 \tag{39}$$

assuming that load impedance $Z_{load}(0)$=0 vanishes at low frequencies and the input current $i$=0.

### D.Offset from Symmetry Point

If the armature rest position $x_e$ is identical with the symmetry point $x_s$, the BA-transducer has the highest efficiency and generates minimum 2nd-, 4th and other even-order harmonic distortion. The offset $x_{off} = x_e - x_s$ is a meaningful characteristic for adjusting the equilibrium rest position $x_e$.

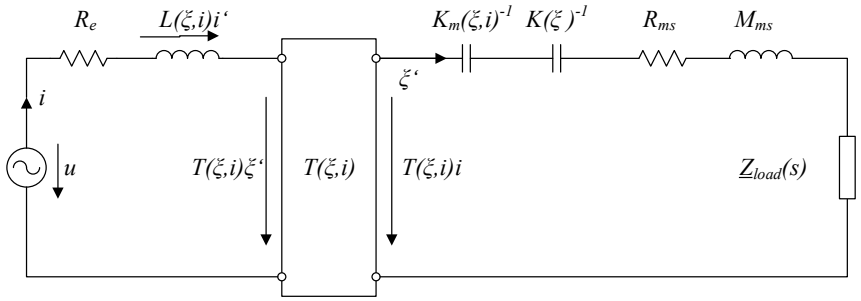


*Figure 8. Equivalent circuit of the extended model considering the displacement ξ from the equilibrium position xe*

## V. ARMATURE DISPLACEMENT

The displacement $\xi = x - x_e$ of the armature from the equilibrium rest position $x_e$ is the most important internal state variable because it that generates both the acoustical output and the back EMF at the terminals via velocity.

Therefore, it is useful in practice to exchange the position $x$ in Eqs. (40) and (41) by the displacement $\xi$, giving the voltage equation

$$u = R_e i + L(\xi,i)\frac{di}{dt} + T(\xi,i)\frac{d\xi}{dt} \tag{40}$$

and force equation

$$\begin{aligned} T(\xi,i)i = &\left(K(x_e+\xi) - K(x_e)\right)\xi \\ &- K_\phi(\xi,i)\xi \\ &+ \mathrm{L}^{-1}\left[\underline{Z}_m(\xi,s)s\right] * \xi \end{aligned} \tag{41}$$

corresponding to the equivalent circuit shown in Figure 8. The nonlinear inductance can be expressed as

$$L(\xi,i) = Lf_\xi\left(\xi,i\right) \tag{42}$$

using the small signal value of the inductance at the equilibrium position $x_e$

$$\begin{aligned} L = L_x(x_e, i=0) &= L_x(x_s + x_{off}, i=0) \\ &= L_s f_x\left(x_s + x_{off}, i=0\right) \\ &= L_s f_\xi\left(\xi=0, i=0\right) \end{aligned} \tag{43}$$

and the flux function $f_\xi(\xi,i)$ depending on displacement $\xi$ and current $i$:

$$f_\xi(\xi,i)=\frac{1}{1-\left(\frac{\xi-x_{off}}{D}\right)^2+\sum_{k=1}^{K}s_k\left|i+s_x\left(\frac{\xi-x_{off}}{D}\right)\right|^k} \tag{44}$$

The mechanical stiffness of the mechanical suspension developed into a power series is

$$K(x_e+\xi)=K_{ms}+\sum_{k=1}^{K}k_k\xi^k \tag{45}$$

with the linear stiffness parameter $K_{ms}$.

The nonlinear electro-magnetic transduction factor can be expressed as

$$T(\xi,i)=Tf_\xi(\xi,i) \tag{46}$$

with linear transduction factor $T$ at the equilibrium position:

$$T=T_x(x_e,i=0)=\lambda L f_\xi(\xi=0,i=0) \tag{47}$$

The magnetic stiffness becomes

$$K_\phi(\xi,i)=K_\phi f_\xi(\xi,i) \tag{48}$$

using the small signal value $K_\phi$ at equilibrium position $x_e$:

$$K_\phi=K_{\phi x}(x_e,i=0)=-\lambda^2 L f_\xi(\xi=0,i=0) \tag{49}$$

## A.Free Model Parameters

The nonlinear model describing the armature displacement in section V uses a minimum number of free parameters summarized in

$$\begin{aligned}\mathbf{P}&=\begin{bmatrix}\mathbf{P}_{lin} & \mathbf{P}_{nlin}\end{bmatrix}\\&=\begin{bmatrix}\mathbf{P}_{lin} & \mathbf{P}_{mag} & \mathbf{P}_{sus}\end{bmatrix}\end{aligned} \tag{50}$$

comprising linear parameters valid at small amplitudes $i\approx0$ and $\xi\approx0$

$$\mathbf{P}_{lin}=\begin{bmatrix}R_e & M_{ms} & L_e & R_{ms} & \lambda & K_{ms}\end{bmatrix} \tag{51}$$

and nonlinear parameters $\mathbf{P}_{nlin}$ which can be separated into parameters of the magnetic circuit

$$\mathbf{P}_{mag}=\begin{bmatrix}x_{off} & s_x & D_{eff} & s_1 & \dots & s_K\end{bmatrix} \tag{52}$$

and parameters of the mechanic or acoustic suspension (equivalent air stiffness in a sealed enclosure):

$$\mathbf{P}_{sus}=\begin{bmatrix}k_1 & \dots & k_K\end{bmatrix} \tag{53}$$

The linear parameters $\mathbf{P}_{\mathrm{lin}}$ can be identified at small amplitudes based on the electrical impedance $Z_e(f)$ using conventional perturbation techniques (e.g. with and without added mass), laser vibrometry for measuring displacement or other time derivates. The parameters resistance $R_e$, moving mass $M_{ms}$, inductance $L_e$, mechanical resistance $R_{ms}$ and mechanical stiffness $K_{ms}$ are also found in electro-dynamical transducers. The parameter $\lambda$ is unique in BA-transducers and describes the relationship between inductance $L$ and transduction parameter $T$. The nonlinear suspension parameters $\mathbf{P}_{\mathbf{sus}}$ can be measured by static or dynamic measurement techniques defined in the IEC standard 62457 [8].

The nonlinear magnetic parameters $\mathbf{P}_{mag}$ define the flux function $f_\xi(\xi,i)$ which generates a similar nonlinear curve shape in the inductance $L(\xi,i)$, transduction factor $T(\xi,i)$ and magnetic stiffness $K_\phi(\xi,i)$. Based on the theory developed in this paper, a system identification technique

as defined in IEC standard 62458 [9] can also be developed for those parameters. The parameters **P** have a high diagnostic value for assessing design choices during the development process. The information is also useful for manufacturing and quality control. The offset $x_{off}=x_s-x_e$, for example, is a meaningful characteristic for adjusting an armature's equilibrium position $x_e$.

## VI. CONCLUSIONS

The paper presented a nonlinear model of the balanced armature transducer that considers the geometry and the material properties of the magnetic system. The new model uses the conventional theory as a starting point but additionally considers the saturation in soft iron parts and asymmetries in the nonlinear parameter shape caused by an offset in the armature rest position, different magnetization of the two magnets and other physical causes. This new model is the basis for numerical simulations to predict fundamental response, armature position, maximum output (e.g. $SPL_{max}$), the even- and odd-order harmonic and intermodulation distortion and to assess the stability of the BA-transducer. However, those simulations and investigations on design choices need accurate input parameters, which can be provided for virtual design choices by finite element analysis (FEA) or real transducers by system identification techniques.

The accuracy of the model can be evaluated by comparing measured transfer functions and distortion data (e.g. THD) with predicted values. The model can be further improved by introducing additional parameters describing the losses in the inductance, in the mechanical suspension and in the air flow at the outlet in the front volume. However, a model with minimum complexity but sufficient accuracy is preferred for designing nonlinear control systems for BA-transducers.

## VII. REFERENCES


[1] L. Beranek, T. Mellow, "Acoustics: Sound Field and Transducers," Academic Press, Amsterdam, 2012.

[2] F.V. Hunt, „Electroacoustics – The Analysis of Transduction and Its Historical Background, "(Acoustical Society of America, New York, 1954, 1982), chap. 7.

[3] R. Carlisle, "History and Current Status of Miniature Variable-Reluctance Balanced-Armature Transducer," J. Audio Eng. Volume **13**, January 1965, pp. 45 -49.

[4] J. Jensen, et. al. „Nonlinear Time-Domain Modeling of Balanced-Armature Receivers, "J. Audio Eng. Soc. **59**, No.3, (2011).

[5] W. Klippel, "Anordnung und Verfahren zur Identifikation und Korrektur der nichtlinearen Eigenschaften elektromagnetischer Wandler," patent DE 201310012811, (filed August 2013).

[6] J. Jensen, Nonlinear Distortion Mechanisms and Efficiency of Miniature Balance-Armature Loudspeakers, "PhD thesis, Technical University of Denmark, Lyngby, Denmark, (2014).

[7] S. Thompson, "Methods and Apparatus for Reduced Distortion Balanced Armature Devices, US patent 8,385,583, (Feb. 2009).

[8] Sound system equipment - Electroacoustical transducers - Measurement of suspension parts, IEC 62459:2010.

[9] Sound System Equipment – Electro-acoustical Transducers – Measurement of Large Signal Parameters, IEC 62458:2010.

[10] W. Klippel, "Nonlinearities in Balanced Armature Transducers, "J. of the Acoustical Soc. of America 148(1):25- 32, July 2020, DOI: 10.1121/10.0001496